

## P–V–T equation of state of $\text{Ca}_3\text{Al}_2\text{Si}_3\text{O}_{12}$ grossular garnet

Steeve Gréaux · Yoshio Kono · Norimasa Nishiyama · Takehiro Kunimoto · Kouhei Wada · Tetsuo Irifune

Received: 18 March 2010/Accepted: 14 June 2010/Published online: 29 June 2010  
© Springer-Verlag 2010

**Abstract** The thermoelastic parameters of synthetic  $\text{Ca}_3\text{Al}_2\text{Si}_3\text{O}_{12}$  grossular garnet were examined in situ at high-pressure and high-temperature by energy dispersive X-ray diffraction, using a Kawai-type multi-anvil press apparatus coupled with synchrotron radiation. Measurements have been conducted at pressures up to 20 GPa and temperatures up to 1,650 K: this  $P$ ,  $T$  range covered the entire high- $P$ ,  $T$  stability field of grossular garnet. The analysis of room temperature data yielded  $V_{0,300} = 1,664 \pm 2 \text{ \AA}^3$  and  $K_0 = 166 \pm 3 \text{ GPa}$  for  $K'_0$  fixed to 4.0. Fitting of our  $P$ – $V$ – $T$  data by means of the high-temperature third order Birch–Murnaghan or the Mie–Grüneisen–Debye thermal equations of state, gives the thermoelastic parameters:  $(\partial K_{0,T}/\partial T)_P = -0.019 \pm 0.001 \text{ GPa K}^{-1}$  and  $\alpha_{0,T} = 2.62 \pm 0.23 \times 10^{-5} \text{ K}^{-1}$ , or  $\gamma_0 = 1.21$  for fixed values  $q_0 = 1.0$  and  $\theta_0 = 823$  (Isaak et al. Phys Chem Min 19:106–120, 1992). From the comparison of fits from two different approaches, we propose to constrain the bulk modulus of grossular garnet and its pressure derivative to  $K_{T0} = 166 \text{ GPa}$  and  $K'_{T0} = 4.03\text{--}4.35$ . Present results are compared with previously determined thermoelastic properties of grossular-rich garnets.

**Keywords** Thermal expansion · Grossular garnet · High-pressure · In situ X-ray diffraction

### Introduction

Silicate garnets are counted as one of the most abundant constituent minerals of the Earth's mantle transition zone rising up to 40 vol% for pyrolite composition, and up to 60 vol% for piclogite composition (Bass and Anderson 1984; Irifune and Ringwood 1987). Garnets are also important constituents of subducted oceanic crust, and it is suggested that garnet-rich subducted crust can be gravitationally trapped in the lowermost part of the mantle transition zone (Irifune and Ringwood 1993; Karato et al. 1995). Furthermore, recent seismological observations showed occurrences of multiple discontinuities, which might be the result of post-garnet transformations (e.g. Deuss et al. 2006; Saikia et al. 2008). Thus, garnets are believed to play a significant role in the nature and dynamics of shallower to middle parts of the Earth's mantle, and therefore the determination of the  $P$ – $V$ – $T$  properties of garnets is of importance to infer the appropriate mineralogical and compositional model in this region.

$\text{X}_3\text{Y}_2\text{Z}_3\text{O}_{12}$  garnets have an internal centered cubic lattice (space group  $Ia\bar{3}d$ ), which displays dodecahedral (X), octahedral (Y), and tetrahedral (Z) crystallographic sites. This unique feature makes the garnet structure flexible in accommodating a variety of cations with different ionic radii. In Earth relevant compositions, garnet are mostly present as a non ideal solid solution where  $\text{X} = \text{Mg}^{2+}$ ,  $\text{Fe}^{2+}$ ,  $\text{Ca}^{2+}$ ,  $\text{Mn}^{2+}$ ;  $\text{Y} = \text{Al}^{3+}$ ,  $\text{Fe}^{3+}$ ,  $\text{Cr}^{3+}$ ;  $\text{Z} = \text{Si}^{4+}$ . Therefore, as the chemical composition of natural garnets can be complex and might significantly vary in the mantle from one region to another, the study of thermoelastic properties of garnet end-members at high-pressure and high-temperature is an important step to understand the behavior of complex garnet compositions in the Earth.

S. Gréaux (✉) · Y. Kono · N. Nishiyama · T. Kunimoto · K. Wada · T. Irifune  
Geodynamics Research Center, Ehime University,  
4-5 Bunkyo-cho, Matsuyama 790-8577, Ehime, Japan  
e-mail: greaux@sci.ehime-u.ac.jp

T. Kunimoto  
JASRI, 1-1-1 Mikazuki-cho, Sayo-gun, Hyogo 679-5198, Japan

Grossular garnet of composition  $\text{Ca}_3\text{Al}_2\text{Si}_3\text{O}_{12}$  (ugrandite group) is one of the most significant calcium end-member of the mantle garnets. The crystal structure of grossular species has been extensively studied at room  $P$ ,  $T$  conditions (Meagher 1975; Novak and Gibbs 1971; Rodehorst et al. 2002; Sawada 1999). Nevertheless, to date, most of the studies about grossular garnet thermoelastic properties under high  $P$ ,  $T$  conditions have been limited, either to high temperature and ambient pressure (Isaak et al. 1992; Thiéblot et al. 1998, 1999), or to high pressure and room temperature (Conrad et al. 1999; Hazen and Finger 1978; Olijnyk et al. 1991; Zhang et al. 1999). In fact, relatively few studies have been able to measure thermoelastic properties of grossular garnet *in situ* at simultaneous high-pressure and high-temperature. Pavese et al. (2001) investigated the pressure–volume–temperature dependence of natural grossular-rich garnet composition by X-ray powder diffraction, using a Paris–Edinburgh press apparatus up to 5 GPa and 1,000 K. Their work showed relatively good agreement with  $K_0$  values attained using different techniques with the exception of the results of Zhang et al. (1999); and then discrepancies were ascribed to the use of natural samples from different origin (i.e. different composition). In contrast, Pavese et al. (2001) reported  $K'_0$  close to 3.0, which differ from a previous determination of  $K'_0$  which was higher than 5.0 (Conrad et al. 1999; Olijnyk et al. 1991; Zhang et al. 1999). In addition, bulk thermal expansion deviates significantly from values reported by former studies (Anderson and Isaak 1995; Isaak et al. 1992; Skinner 1956). In addition, the  $P$ – $T$  range of Pavese et al. (2001) is narrow compared to the wide stability field of garnet ( $P$  up to ~20 GPa). In fact, high- $P$ ,  $T$  thermoelastic data of the grossular garnet end-member are still not completely well constrained.

Here, we investigated the pressure–volume–temperature relation of synthetic  $\text{Ca}_3\text{Al}_2\text{Si}_3\text{O}_{12}$  grossular garnet by means of multi-anvil press experiments coupled with Energy Dispersive X-Ray Diffraction (EDXRD) using the synchrotron radiation at the beamline BL04B1 (SPring-8, Japan). The use of a large-volume apparatus permits precise control of experimental conditions over a large range of pressure and temperature (Rubie 1998). Energy

dispersive powder diffraction pattern profiles were measured *in situ* simultaneously at high-pressure and at high-temperature (up to 20 GPa and 1,650 K) covering the entire stability field of grossular garnet as minor peaks of  $\text{CaSiO}_3$  perovskite start to be observed at the highest  $P$ ,  $T$  conditions. Our results are presented and discussed with respect to previous works, up to the  $P$ ,  $T$  conditions of the middle-part of the mantle transition zone.

## Experimental methods

Starting materials were prepared by mechanical mix of commercial oxides in the molar proportions:  $3\text{CaCO}_3 \cdot 1\text{Al}_2\text{O}_3 \cdot 3\text{SiO}_2$  and placed one night at 1,173 K for removing carbonates. The mixture was then melted at ~1,973 K (Osborn and Muan 1960) which produced, after quench, a homogeneous glass with the following composition (in wt%):  $\text{CaO}$ , 37.14;  $\text{Al}_2\text{O}_3$ , 21.12;  $\text{SiO}_2$ , 40.70. Crystalline grossular was synthesized from the latter glass at ~7 GPa and 1,673 K during 2 h using a Kawai-type multi-anvil press apparatus (MAP) at the Geodynamics Research Center (Ehime University, Matsuyama, Japan). SEM-EDX analysis yielded the composition of grossular garnet as follows (in wt%):  $\text{CaO}$ , 36.84;  $\text{Al}_2\text{O}_3$ , 22.35;  $\text{SiO}_2$ , 40.80, which can also be written in term of formula unit as:  $\text{Ca}_{2.95}\text{Al}_{1.97}\text{Si}_{3.04}\text{O}_{12}$ . X-ray diffraction profiles collected prior to HP-HT experiments confirmed grossular garnet with the lattice parameter of  $a_0 = 11.8442 \pm 0.0003 \text{ \AA}$  (space group  $Ia\bar{3}d$ ) that is in fair agreement with previous studies (Table 1) (Meagher 1975; Novak and Gibbs 1971; Rodehorst et al. 2002; Sawada 1999).

High-pressure and high-temperature *in situ* experiments were carried out using a Kawai-type multi-anvil press apparatus, SPEED-1,500, located at the beamline BL04B1 that operates at the synchrotron radiation facility, SPring-8 (Hyogo Prefecture, Japan). High-pressure was generated within so called 8/2.5 assemblies, which consist in a Co-doped  $\text{MgO}$  octahedron pressure medium, with a side-length of 8 mm; and tungsten carbide anvils with a 2.5 mm truncation edge-length, supported by pyrophyllite gaskets that were used to compress the cell assembly. A cylindrical

**Table 1** Comparison of lattice parameters of grossular garnet at ambient  $P$ ,  $T$  conditions

Grossular composition	$a_0$ (Å)	$V_0$ (Å $^3$ )	Reference
Synthetic $\text{Ca}_3\text{Al}_2\text{Si}_3\text{O}_{12}$	11.8442 (3)	1,661.6 (1)	This study
( $\text{Ca}_{2.96}\text{Mn}_{0.04}$ )( $\text{Al}_{1.95}\text{Fe}_{0.05}$ ) $\text{Si}_3\text{O}_{12}$	11.845 (1)	1,661.9 (4)	Novak and Gibbs (1971)
( $\text{Ca}_{2.96}\text{Mn}_{0.04}$ )( $\text{Al}_{1.95}\text{Fe}_{0.05}$ ) $\text{Si}_3\text{O}_{12}$	11.846 (2)	1,662.3 (8)	Meagher (1975)
Natural $\text{Ca}_3\text{Al}_2\text{Si}_3\text{O}_{12}$	11.8504 (4)	1,664.2 (2)	Sawada (1999)
Synthetic $\text{Ca}_3\text{Al}_2\text{Si}_3\text{O}_{12}$	11.8502 (4)	1,664.1 (2)	Rodehorst et al. (2002)

Numbers in parenthesis represent the relative error calculated for  $a$  and  $V$

$\text{LaCrO}_3$  heater equipped with  $\text{ZrO}_2$  insulators and molybdenum electrodes was used to generate high-temperature during the experiments at high-pressure. Holes of 1.0 mm in diameter, filled with graphite windows were made through the furnace, for an X-ray path. Temperature was measured by means of  $\text{W}_{97}\text{Re}_3$ – $\text{W}_{75}\text{Re}_{25}$  thermocouple, which was maintained between the capsule and an  $\text{MgO}$  sleeve that served as soft pressure transmitting medium inside of the furnace. Capsules consisted of cylindrical graphite with gold foil at each ends. Crystalline grossular garnet was powdered beforehand and mechanically mixed with gold powder as the pressure calibrant (1/10th of sample's weight) then loaded within the capsule. In addition, we added the X-ray diffraction data collected using a 14/7 assembly, which was simultaneously obtained with ultrasonic measurement for the polycrystalline grossular at pressures up to 16.4 GPa and temperatures up to 1,650 K (Kono et al. unpublished data). We used tungsten carbide anvils with a TEL of 7 mm and Co-doped  $\text{MgO}$  octahedron pressure medium with an edge length of 14 mm. Platinum foil tube heaters were used in this cell assembly.  $\text{LaCrO}_3$  sleeve was used as a thermal insulator, and  $\text{MgO}$  window was placed in the  $\text{LaCrO}_3$  sleeve for obtaining X-ray diffraction of the sample. We used  $\text{MgO}$  and  $\text{NaCl}$  sleeves as the sample container to realize a quasi-hydrostatic environment. Details of the experimental setup and cell assembly were described in Higo et al. (2009). Pressure during all in situ measurements was calculated after the gold equation of state as described by (Tsuchiya 2003).

A set of 6 high-pressure and high-temperature experiments were performed, in the  $P$ ,  $T$  range of 0.0–19.6 GPa and 300–1,650 K (see Fig. 1; Table 2). Run S1839 and S1850 were for each pressure, annealed at  $T$  higher than

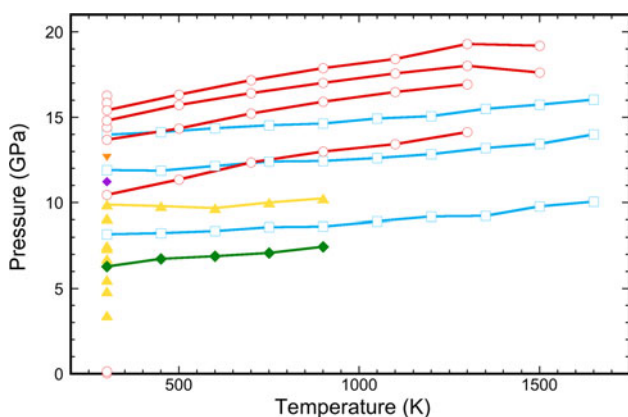


**Fig. 1** Pressure–temperature conditions during in situ measurements at high  $P$ ,  $T$  of grossular garnet. Purple diamond Run S1839, Orange inverse triangle Run S1850, Yellow triangles Run S1851, Green diamonds Run S1885, Open blue squares Run S1886, Open red circles Run S2188. Each symbol represents a  $P$ ,  $T$  condition where XRD profile of  $\text{Ca}_3\text{Al}_2\text{Si}_3\text{O}_{12}$  grossular garnet was taken

1,000 K then quenched to room temperature where X-ray profiles were collected. Run S1851 and S1885 were pressurized to  $\sim 7.5$  and  $\sim 10.5$  GPa, respectively, and heated to 900 K, after then data were collected upon decrease of temperature to 300 K in steps of 150 K. One can note that for run S1851 additional data were collected at 300 K during decompression. Run S1886 was first pressurized to  $\sim 11.0$  GPa, heated up to 1,650 K then data were collected during decreasing temperature to 300 K by steps of 150 K. Following this, the pressure was increased to 14.5 GPa then 16.9 GPa, and the same heating/collecting data procedure is repeated at each  $P$ -step. The same overall procedure was applied to run S2188 at 14.1 GPa, 16.9 GPa, 17.6 and 19.1 GPa successively (4  $P$ -steps in total). Maximum heating temperature was about 1,300 K in the two-first steps, and 1,500 K in the two last ones; then X-ray diffraction profiles were collected to 300 K in steps of 200 K.

Figure 2 shows an EDXRD profile collected at 10.4 GPa and 300 K. Analyzes of all the patterns were carried out for the range of 35–115 keV by means of the multiphase profile-fitting technique implemented in the EXPGUI/GSAS software package (Larson and Von Dreele 2000; Toby 2001). Refinement of peak positions and extraction of cell parameters were achieved by reducing full diffraction patterns following the LeBail method (Le Bail et al. 1988). Precision upon the volume for both grossular garnet and gold (pressure marker) was estimated from the Lebail refinement of X-ray diffraction profiles, for each experimental profile separately. The precision upon the calculation of the pressure after the equation of state of gold (Tsuchiya 2003) was estimated by taking in account the propagated errors from the uncertainties on the measurement of the unit-cell volume of gold.

## Results and discussion

### Pressure–volume data at room temperature

The volume–pressure relations have been determined at 300 K, from 0.0 to 16.5 GPa. Weighting factors were calculated using the experimental uncertainties in pressure and volume (see Table 2). Fitting to a third-order Birch–Murnaghan equation of state (Fig. 3) was used with the general form as follows:

$$P(V, 300) = \frac{3}{2} K_{0,300} \times \left[ \left( \frac{V_{0,300}}{V_{P,300}} \right)^{\frac{2}{3}} - \left( \frac{V_{0,300}}{V_{P,300}} \right)^{\frac{5}{3}} \right] \\ \times \left\{ 1 - \frac{3}{4} \left( 4 - K'_{0,300} \right) \times \left[ \left( \frac{V_{0,300}}{V_{P,300}} \right)^{\frac{2}{3}} - 1 \right] \right\} \quad (1)$$

**Table 2** Pressure, temperature, lattice parameter and unit cell volume of grossular garnet

P (GPa)	T (K)	a (Å)	V (Å <sup>3</sup> )	P (GPa)	T (K)	a (Å)	V (Å <sup>3</sup> )
Run S1851				Run S1839			
10.68 (3)	900	11.6669 (5)	1,588.07 (21)	11.47 (2)	300	11.6126 (3)	1,566.01 (12)
10.19 (3)	750	11.6642 (4)	1,586.95 (15)	Run S1850			
9.83 (3)	600	11.6589 (4)	1,584.79 (16)	12.69 (1)	300	11.5873 (3)	1,555.79 (12)
9.75 (3)	450	11.6524 (4)	1,582.16 (16)	14.09 (2)	300	11.5674 (3)	1,547.77 (13)
9.95 (2)	300	11.6452 (3)	1,579.22 (13)	14.82 (2)	300	11.5581 (3)	1,544.06 (13)
7.26 (2)	300	11.6937 (3)	1,599.03 (12)	Run S1885			
9.17 (2)	300	11.6606 (3)	1,585.50 (11)	7.64 (2)	900	11.7237 (3)	1,611.37 (15)
7.54 (3)	300	11.6878 (3)	1,596.61 (11)	7.24 (2)	750	11.7211 (3)	1,610.28 (14)
6.76 (3)	300	11.7004 (3)	1,601.80 (14)	6.95 (1)	600	11.7137 (5)	1,607.23 (21)
5.39 (2)	300	11.7173 (3)	1,608.72 (12)	6.68 (1)	450	11.7075 (5)	1,604.70 (20)
4.93 (2)	300	11.7465 (3)	1,620.79 (12)	6.12 (2)	300	11.7068 (2)	1,604.43 (8)
3.45 (2)	300	11.7668 (3)	1,629.22 (13)	Run S2188			
Run S1886				0.00 (2)	300	11.8442 (3)	1,661.58 (12)
10.71 (1)	1,650	11.7447 (5)	1,620.02 (22)	16.27 (6)	300	11.5385 (15)	1,536.22 (63)
10.09 (1)	1,500	11.7395 (5)	1,617.89 (20)	14.14 (4)	1,300	11.6446 (8)	1,578.97 (35)
9.52 (3)	1,350	11.7301 (4)	1,613.99 (15)	13.42 (4)	1,100	11.6436 (3)	1,578.57 (10)
9.38 (4)	1,200	11.7228 (3)	1,611.01 (14)	12.98 (3)	900	11.6377 (2)	1,576.18 (10)
9.40 (3)	1,050	11.7150 (3)	1,607.79 (12)	12.35 (5)	700	11.6320 (2)	1,573.83 (9)
9.15 (2)	900	11.7072 (3)	1,604.59 (14)	11.35 (2)	500	11.6256 (2)	1,571.25 (10)
8.87 (3)	750	11.6981 (4)	1,600.85 (17)	10.45 (2)	300	11.6216 (2)	1,569.64 (9)
8.59 (4)	600	11.6905 (4)	1,597.53 (17)	14.41 (5)	300	11.5586 (4)	1,544.23 (16)
8.47 (3)	450	11.6860 (3)	1,595.86 (12)	16.93 (3)	1,300	11.5965 (2)	1,559.48 (6)
8.44 (4)	300	11.6837 (4)	1,594.93 (16)	16.47 (2)	1,100	11.5885 (2)	1,556.25 (10)
14.46 (2)	1,650	11.6614 (3)	1,585.82 (10)	15.91 (2)	900	11.5818 (2)	1,553.58 (9)
14.06 (1)	1,500	11.6562 (2)	1,583.70 (10)	15.22 (3)	700	11.5759 (2)	1,551.20 (9)
13.79 (1)	1,350	11.6492 (3)	1,580.86 (11)	14.33 (2)	500	11.5679 (3)	1,547.98 (11)
13.35 (1)	1,200	11.6432 (2)	1,578.39 (10)	13.69 (2)	300	11.5640 (3)	1,546.41 (11)
13.01 (1)	1,050	11.6432 (2)	1,578.40 (10)	16.28 (5)	300	11.5272 (2)	1,531.68 (10)
12.77 (1)	900	11.6291 (3)	1,572.68 (12)	17.61 (2)	1,500	11.5893 (2)	1,556.58 (10)
12.56 (1)	750	11.6212 (3)	1,569.47 (12)	18.02 (2)	1,300	11.5813 (2)	1,553.35 (10)
12.40 (2)	600	11.6154 (3)	1,567.12 (10)	17.56 (2)	1,100	11.5761 (4)	1,551.27 (17)
12.09 (2)	450	11.6084 (2)	1,564.29 (10)	17.02 (2)	900	11.5698 (4)	1,548.72 (16)
11.82 (3)	300	11.6035 (2)	1,562.29 (9)	16.42 (2)	700	11.5555 (2)	1,543.02 (9)
16.91 (3)	1,650	11.6227 (4)	1,570.10 (16)	15.71 (2)	500	11.5541 (3)	1,542.46 (13)
16.64 (2)	1,500	11.6164 (4)	1,567.54 (15)	14.81 (2)	300	11.5542 (3)	1,542.49 (12)
16.37 (2)	1,350	11.6108 (4)	1,565.27 (17)	15.86 (4)	300	11.5302 (3)	1,532.90 (11)
16.00 (2)	1,200	11.6052 (4)	1,562.98 (15)	19.19 (4)	1,500	11.5605 (4)	1,544.99 (17)
15.64 (2)	1,050	11.5979 (4)	1,560.06 (15)	19.3 (4)	1,300	11.5581 (5)	1,544.06 (18)
15.13 (2)	900	11.5909 (3)	1,557.21 (12)	18.42 (4)	1,100	11.5513 (4)	1,541.33 (17)
14.92 (3)	750	11.5858 (4)	1,555.17 (15)	17.88 (3)	900	11.5446 (4)	1,538.63 (16)
14.78 (3)	600	11.5793 (4)	1,552.55 (15)	17.17 (3)	700	11.5386 (4)	1,536.24 (17)
14.54 (3)	450	11.5734 (4)	1,550.20 (15)	16.33 (3)	500	11.5313 (4)	1,533.33 (16)
14.27 (4)	300	11.5670 (3)	1,547.61 (11)	15.41 (3)	300	11.5294 (4)	1,532.55 (17)
				0.00 (2)	300	11.8458 (4)	1,662.22 (16)

Numbers in parenthesis represent the relative error calculated for  $a$ ,  $V$  and  $P$

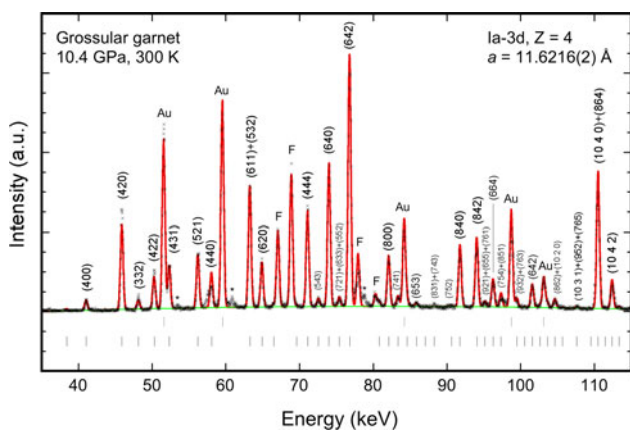


**Fig. 2** Example of Energy Dispersive X-Ray Diffraction profile collected for  $\text{Ca}_3\text{Al}_2\text{Si}_3\text{O}_{12}$  grossular garnet (10.4 GPa and 300 K, angle = 5.961°). Black crosses experimental data, Red line Le Bail fit, Green line background fit. Peak positions are indicated for gold (Au, upper bars) and grossular garnet (Miller indices, lower bars). Gold fluorescence and minor unidentified peaks are marked by “F” and \*, respectively

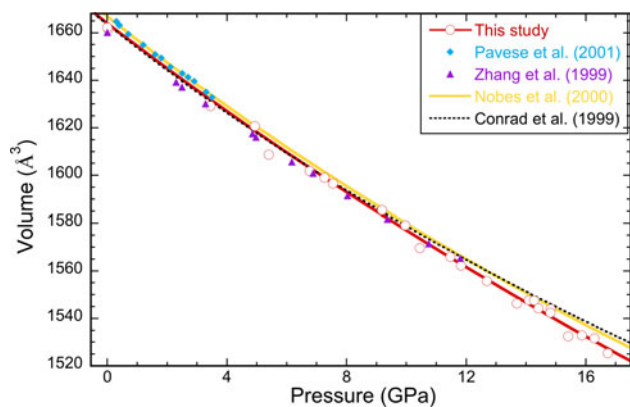


**Fig. 3** Compression data of  $\text{Ca}_3\text{Al}_2\text{Si}_3\text{O}_{12}$  grossular garnet at room temperature. Open circles represent the present data points. The red open circles and plain line are our data fitted to the third-order Birch–Murnaghan equations of state ( $K_{0,300} = 166$  (3) GPa and  $K'_{0,300} = 4.0$ ). Blue diamonds and purple triangles are experimental points at 300 K from Pavese et al. (2001) and Zhang et al. (1999), respectively. Dashed black line and yellow plain line are from Conrad et al. (1999) ( $K_{0,300} = 165.68$  GPa and  $K'_{0,300} = 5.46$ ) and Nobes et al. (2000) ( $K_{0,300} = 166$  GPa and  $K'_{0,300} = 4.3$ ) respectively. Volume and pressure uncertainties estimated from the X-ray diffraction profiles are about the same size of the symbols

where  $K_{0,300}$ ,  $K'_{0,300}$  and  $V_{0,300}$  are the isothermal bulk modulus, its pressure derivative and the unit cell volume at room  $P$ ,  $T$  conditions, respectively. When  $K'_{0,300}$  is fixed to 4.0, fitting of Eq. 1 gives  $K_{0,300} = 166 \pm 3$  GPa and  $V_{0,300} = 1,664 \pm 2 \text{ Å}^3$  ( $\chi^2 = 1.08$ , Table 3). The  $P$ – $V$  relation is in good agreement with previous studies for garnets with grossular-like composition (Hazen and Finger 1978; Nobes et al. 2000; Pavese et al. 2001) (Fig. 3). However, in the case of Conrad et al. (1999), their  $K_{0,300}$

value of about 166 GPa is associated with a higher  $K'_{0,300}$  of 5.46. As shown on Fig. 3, at low-pressure our  $P$ – $V$  relation agrees well with Conrad et al. (1999). However, they carried out experiments up to 10 GPa, and then significant deviations with our data arise above  $\sim 10$  GPa because of their high  $K'_{0,300}$  value. Zhang et al. (1999) also reported a similar  $K'_{0,300}$  of  $5.2 \pm 0.6$  but their  $K_{0,300}$  is significantly higher than other studies. Among previous experimental studies, Zhang et al. (1999) reported the lowest  $V_{0,300} = 1,660.2 \pm 0.1 \text{ Å}^3$  (see Table 3). Figure 3 shows that original  $P$ – $V$  data of Zhang et al. (1999) agrees well with our data with the exception of its  $V_{0,300}$ : it is likely that discrepancies in their  $K_{0,300}$  and  $K'_{0,300}$  values could be related to the difference of  $V_0$  between our studies. Fitting of Eq. 1 with  $K'_{0,300}$  as a free parameter and  $V_{0,300}$  fixed to  $1,664 \text{ Å}^3$ , leads to a bulk modulus of  $K_{0,300} = 172 \pm 2$  GPa, with a pressure derivative,  $K'_{0,300} = 3.00 \pm 0.75$  ( $\chi^2 = 1.09$ , Table 3) that is significantly lower than the value of Zhang et al. (1999). Pavese et al. (2001) reported refined  $K'_{0,300}$  values of  $2.80 \pm 1.91$  and  $3.4 \pm 1.8$  for  $K_{0,300}$  equal to  $167.4 \pm 2.4$  GPa and  $168.6 \pm 2.0$  GPa, respectively. Indeed large uncertainties in their  $K'_{0,300}$  values make agreements difficult to discuss with respect to other studies.

The zero-pressure volume  $V_{0,300}$  is calculated from fitting equation 2, with  $K'_{0,300}$  fixed to 4.0 (see Table 3). The result of  $V_{0,300} = 1,664 \pm 2 \text{ Å}^3$ , is about  $\sim 0.2\%$  larger than the volume measured from fitting X-Ray diffraction profile at ambient pressure ( $V_0 = 1,661.6 \pm 0.1 \text{ Å}^3$ , Table 1). These values are in good agreement with pressure–volume data on natural specimen (Conrad et al. 1999; Pavese et al. 2001). First principle works (Nobes et al. 2000) reported a larger value than our study as it is expected for calculations under the generalized gradient approximation (GGA).

#### $P$ – $V$ – $T$ data and thermoelastic parameters

Pressure–volume–temperature data were used to determine the thermoelastic properties of grossular garnet up to  $\sim 20$  GPa and 1,650 K. In addition, we used thermal expansion data from Isaak et al. (1992) to calculate the volume at ambient pressure and high temperature. Their group studied the thermal expansion at ambient pressure of a natural sample of grossular containing minor amount of andradite, by dilatometry methods up to 1,000 K. Data of  $\alpha_0$  were extrapolated to 2,000 K for the grossular end-member, after correction of the relative difference of  $\alpha_0$  between grossular and andradite, which is given by Skinner (1956).

The third order  $P$ – $V$ – $T$  Birch–Murnaghan equation of state was applied to all our data, including those obtained at room  $P$ ,  $T$  conditions; fit of the data at high-pressure and high-temperature was processed with the form as follows:

**Table 3** Summary of lattice and elastic parameters at ambient pressure and room temperature of grossular garnet for this study, compared to previous studies

Grossular composition/ <i>P, T</i> conditions	<i>V</i> <sub>0,300</sub> (Å <sup>3</sup> )	<i>K</i> <sub>0,300</sub> (GPa)	<i>K'</i> <sub>0,300</sub>	$\chi^2$	Methods	Reference
Synthetic Ca <sub>3</sub> Al <sub>2</sub> Si <sub>3</sub> O <sub>12</sub> <i>P</i> = 0–20 GPa, <i>T</i> = 300–1,650 K	1,664 (2)	166 (3)	4.0 <sup>a</sup>	1.08	XRD MAP	This study
Ca <sub>3</sub> Al <sub>2</sub> Si <sub>3</sub> O <sub>12</sub> + 0.5 wt% FeO <i>P</i> = 0–6 GPa, <i>T</i> = 300 K	1,664 <sup>a</sup>	172 (2)	3.0 (7)	1.09		
Natural Ca <sub>3</sub> Al <sub>2</sub> Si <sub>3</sub> O <sub>12</sub> <i>P</i> = 0–12 GPa, <i>T</i> = 300 K	1,660.2 (3)	170 (4)	5.2 (6)	—	XRD DAC	Zhang et al. (1999)
(Ca <sub>2.95</sub> Mg <sub>0.04</sub> Fe <sub>0.01</sub> )(Al <sub>1.97</sub> Ti <sub>0.02</sub> Mn <sub>0.01</sub> )Si <sub>2.99</sub> O <sub>12</sub> <i>P</i> = 0–10 GPa, <i>T</i> = 300 K	1,663.6	165.68	5.46	—	BS DAC	Conrad et al. (1999)
Ca <sub>3</sub> Al <sub>2</sub> Si <sub>3</sub> O <sub>12</sub> <i>P</i> = 0–120 GPa, <i>T</i> = 0 K	1,666.9	166	4.3	—	GGA Calc.	Nobes et al. (2000)
(Ca <sub>2.90</sub> Fe <sub>0.10</sub> )(Al <sub>1.95</sub> Ti <sub>0.04</sub> Mn <sub>0.01</sub> )Si <sub>2.99</sub> O <sub>12</sub> <i>P</i> = 0–5 GPa, <i>T</i> = 300–1,000 K	1,666.4 (4)	167.4 (2.4)	2.80 (1.91)	1.06	XRD P–E	Pavese et al. (2001)
	1,666.1 <sup>a</sup>	168.2 (1.7)	4.0 <sup>a</sup>	1.04		
	1,666.3 (4)	167.1 (2.4)	4.0 <sup>a</sup>	1.05		
	1,666.1 <sup>a</sup>	168.6 (2.0)	3.42 (1.76)	1.06		

XRD X-ray diffraction, MAP multi-anvil press, DAC diamond anvil cell, BS Brillouin scattering, P–E Paris–Edinburgh

Ab initio calculation, GGA generalized gradient approximation

<sup>a</sup> Values that were fixed during data processing

<sup>b</sup> Contains 1.8 wt% of water

$$P(V, T) = \frac{3}{2} \times K_{0,T} \times \left[ \left( \frac{V_{0,T}}{V_{P,T}} \right)^{\frac{2}{3}} - \left( \frac{V_{0,T}}{V_{P,T}} \right)^{\frac{5}{3}} \right] \\ \times \left\{ 1 - \frac{3}{4} \left( 4 - K'_{0,300} \right) \times \left[ \left( \frac{V_{0,T}}{V_{P,T}} \right)^{\frac{2}{3}} - 1 \right] \right\} \quad (2)$$

The temperature dependence of the volume at ambient pressure can be estimated by using the following equation:

$$V_{0,T} = V_{0,300} \times \exp \left[ \int_{300}^T \alpha_{0,x} dx \right] \quad (3)$$

In this expression, the zero-pressure volume at high-temperature  $V_{0,T}$  is formulated by a function of the thermal expansion at zero-pressure  $\alpha_{0,T}$ , which has an empirical assumption of  $\alpha_{0,T} = a_0 + b_0 T$ .

The zero-pressure bulk modulus  $K_{0,T}$  is expressed as a linear function of temperature, its temperature derivative  $(\partial K_{0,T}/\partial T)_P$  and  $K_{0,300}$  as follows:

$$K_{0,T} = K_{0,300} + \left( \frac{\partial K_{0,T}}{\partial T} \right)_P \times (T - 300) \quad (4)$$

Thermoelastic parameters  $\alpha_{0,T}$ ,  $(\partial K_{0,T}/\partial T)_P$  and  $K_{0,300}$  are fitted for the present set of data, with  $K'_{0,300}$  and  $V_{0,300}$  as fixed parameters from our study at room temperature.

Results of the fit of  $\alpha_{0,T}$  and  $(\partial K_{0,T}/\partial T)_P$  are compared, to previous studies on silicate garnets for a set of different  $K'_{0,300}$  fixed values (Table 4). When there is no constraint applied on the elastic parameters, fitting of Eq. 2 gives  $K_{0,300} = 159.7 \pm 4.0$  GPa,  $K'_{0,300} = 5.10 \pm 0.48$ ,  $(\partial K_{0,T}/\partial T)_P = -0.021 \pm 0.002$  GPa K<sup>-1</sup> and  $\alpha_{0,300} = 2.77 \pm 0.24 \times 10^{-5}$  K<sup>-1</sup> ( $\chi^2 = 1.53$ ). As it can be expected, to increase the number of free parameters provides smaller  $\chi^2$ . However, the uncertainties upon the  $K_{0,300}$  and  $K'_{0,300}$  values also increase, which make difficult to discuss those results. This also suggest that even with the large pressure and temperature range covered in this study, the data are not sufficient to constrain all the elastic parameters at the same time during fitting.

On the other hand, when  $K'_{0,300}$  is fixed to 4.0, we obtain  $K_{0,300} = 165.4 \pm 0.8$  GPa,  $(\partial K_{0,T}/\partial T)_P = -0.018 \pm 0.002$  GPa K<sup>-1</sup> and  $\alpha_{0,300} = 2.68 \pm 0.24 \times 10^{-5}$  K<sup>-1</sup> ( $\chi^2 = 1.60$ ) that are of the same order of thermoelastic parameters reported for other garnets. Those results present fair agreement with former results on grossular-rich garnets considering the use of natural samples in previous studies (Anderson and Isaak 1995; Pavese et al. 2001) against synthetic garnet in this work. When fitted with  $K'_{0,300} = 3.0$  or 5.0, the values of  $(\partial K_{0,T}/\partial T)_P$  and  $\alpha_{0,300}$  are almost unaffected. However,  $K_{0,300}$  values (see Table 4) significantly deviate because of the strong correlation between

**Table 4** Results of the fitting by the third order  $P$ – $V$ – $T$  Birch–Murnaghan equation of state of grossular garnet, compared to previous works on other garnet species

	$V_0$ ( $\text{\AA}^3$ )	$K_{0,300}$ (GPa)	$K'_{0,300}$	$(\partial K_{0,T}/\partial T)_P$ (GPa $\text{K}^{-1}$ )	$\alpha_{0,300}$ ( $10^{-5} \text{ K}^{-1}$ )	$a_0$ ( $10^{-5} \text{ K}^{-1}$ )	$b_0$ ( $10^{-8} \text{ K}^{-2}$ )	$\chi^2$
Gr100	1,664*	171.6 (9)	3.0*	−0.017 (1)	2.60 (27)	2.46 (20)	0.48 (24)	1.78
This study	1,664*	165.4 (8)	4.0*	−0.018 (2)	2.68 (24)	2.55 (18)	0.43 (22)	1.60
	1,664*	159.6 (8)	5.0*	−0.020 (2)	2.74 (23)	2.62 (17)	0.40 (20)	1.53
	1,664*	166*	4.03 (13)	−0.019 (1)	2.62 (23)	2.46 (17)	0.54 (21)	1.60
	1,663 (1)	159.7 (40)	5.10 (48)	−0.021 (2)	2.77 (24)	2.65 (18)	0.40 (21)	1.53
(a) Gr97And2Py1	—	166.6 (7)	—	—	1.92 (5)	—	—	—
(b) Gr97Alm3	1,666.08	168.2 (1.7)	4.0*	−0.016 (3)	2.78 (2)	—	—	1.04
(c) Py100	—	170	5.0*	−0.020 (3)	2.3 (2)	—	—	—
(d) Alm100	—	—	—	—	1.62	—	—	—
(e) Alm86Py7Spe7	—	177 (2)	4.0*	−0.032 (16)	3.1 (7)	—	—	—

*Gr*  $\text{Ca}_3\text{Al}_2\text{Si}_3\text{O}_{12}$  grossular, *And*  $\text{Ca}_3\text{Fe}_2\text{Si}_3\text{O}_{12}$  andradite, *Py*  $\text{Mg}_3\text{Al}_2\text{Si}_3\text{O}_{12}$  pyrope, *Alm*  $\text{Fe}_3\text{Al}_2\text{Si}_3\text{O}_{12}$  almandine, *Spe*  $\text{Mn}_3\text{Al}_2\text{Si}_3\text{O}_{12}$  spessartine

References: (a) Isaak et al. (1992); Anderson and Isaak (1995); (b) Pavese et al. (2001); (c) Wang et al. (1998); (d) Thiéblot et al. (1998); (e) Fan et al. (2009)

\* Values that were fixed during data processing

$K_{0,300}$  and  $K'_{0,300}$ , as for fitting of our  $P$ – $V$  data at room temperature. A consistent set of parameters can be obtained by fixing  $K_{0,300}$  to 166 GPa as it is predicted by theoretical work on pure grossular garnet (Nobes et al. 2000), then  $K'_{0,300}$  can be constrained to  $4.03 \pm 0.13$ , which gives  $\alpha_{0,300} = 2.62 \pm 0.23 \times 10^{-5} \text{ K}^{-1}$  and  $(\partial K_{0,T}/\partial T)_P = -0.019 \pm 0.001 \text{ GPa K}^{-1}$  ( $\chi^2 = 1.60$ ). The present  $P$ – $V$ – $T$  measurements have also been fitted using a Vinet-like equation of state. The values we calculated within similar assumptions for the elastic parameters are close to the values obtained from the Birch–Murnaghan model with differences that fall within the uncertainty of the equations of state fits.

Figure 4 shows that for all our fit ( $K'_{0,300}$  fixed to 3.0, 4.0 and 5.0,  $K_{0,300}$  fixed to 166 GPa and fitting with no constraint), the thermal expansion at high-temperature is in fair agreement with Isaak et al. (1992). On the other hand, at low temperature  $\alpha_{0,300}$  is significantly different from that of Isaak et al. (1992) due to the different assumptions in the formulation of  $\alpha_0(T)$ . Thus, we also find smaller values at 300 K than Pavese et al. (2001) who assumed a constant  $\alpha_{0,300}$  value. Figure 5 shows that the temperature dependences of  $K_{0,T}$  for  $K'_{0,300}$  values of about 4.0 are in good agreement with the data of Isaak et al. (1992). Although  $K_{0,T}$  for  $K'_{0,300}$  of 3.0 and 5.0 ( $K'_{0,300} = 5.10 \pm 0.48$  for constraint-free fitting) differ from Isaak et al. (1992),  $(\partial K_{0,T}/\partial T)_P$  values are comparable to those of  $K'_{0,300}$  of 4.0, and the variation of  $K_{0,T}$  is mainly due to the variation of  $K_{0,300}$  with varying  $K'_{0,300}$ . One can note that the present synthetic grossular softens faster against temperature compared to Pavese et al. (2001). The fit of the thermal dilatation of grossular garnet at high-pressure and high-temperature is shown in Fig. 6.

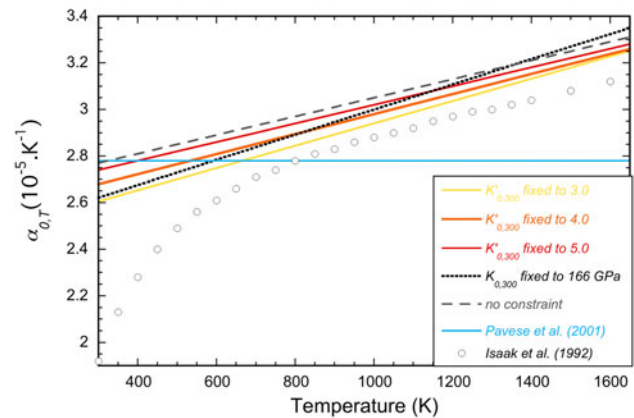


**Fig. 4** Thermal expansion  $\alpha_{0,T}$  against temperature. Solid and dashed lines represent our data for different fixed values of  $K'_{0,300}$  (3.0, 4.0 and 5.0),  $K_{0,300}$  fixed to 166 GPa ( $K'_{0,300} = 4.03 \pm 0.13$ ) and without constraint on the elastic parameters ( $K_{0,300} = 159.7 \pm 4.0 \text{ GPa}$  and  $K'_{0,300} = 5.10 \pm 0.48$ ). Open circles are Isaak et al. (1992) experimental points and the blue line is the constant value of  $\alpha_{0,T}$  as reported by Pavese et al. (2001)

$P$ – $V$ – $T$  data were also analyzed using the so-called Mie–Grüneisen–Debye equation of state (e.g. Jackson and Rigden 1996). In that model, the pressure is expressed as the sum of the static pressure at room temperature and the thermal pressure. The third order Birch–Murnaghan (Eq. 1) and Mie–Grüneisen (Eq. 6) relations are used to, respectively, express the static pressure  $P(V,300)$  and the thermal pressure  $\Delta P_{\text{th}}(V,T)$  as follows:

$$P(V,T) = P(V,300) + \Delta P_{\text{th}}(V,T) \quad (5)$$

$$\Delta P_{\text{th}}(V,T) = \frac{\gamma(V,T)}{V}[E_{\text{th}}(V,T) - E_{\text{th}}(V,T_0)] \quad (6)$$

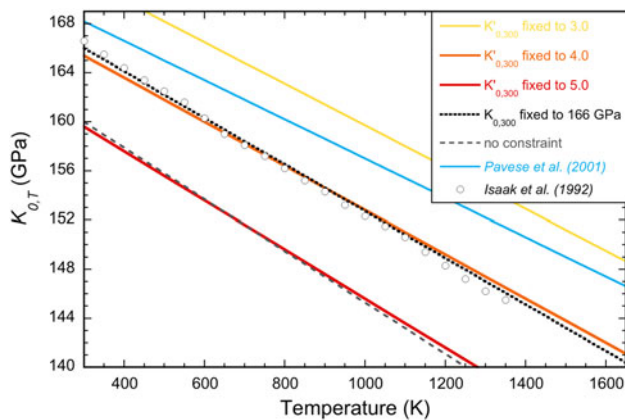


**Fig. 5** Isothermal bulk modulus  $K_{0,T}$  against temperature. Solid and dashed lines represent our data for different fixed values of  $K'_{0,300}$  (3.0, 4.0 and 5.0),  $K_{0,300}$  fixed to 166 GPa ( $K'_{0,300} = 4.03 \pm 0.13$ ) and without constraint on the elastic parameters ( $K_{0,300} = 159.7 \pm 4.0$  GPa and  $K'_{0,300} = 5.10 \pm 0.48$ ). Blue line is plotted after Pavese et al. (2001), for  $K_{0,300} = 168.2 \pm 1.7$  GPa and  $K'_{0,300}$  fixed to 4.0. Open circles are experimental values reported by Isaak et al. (1992)

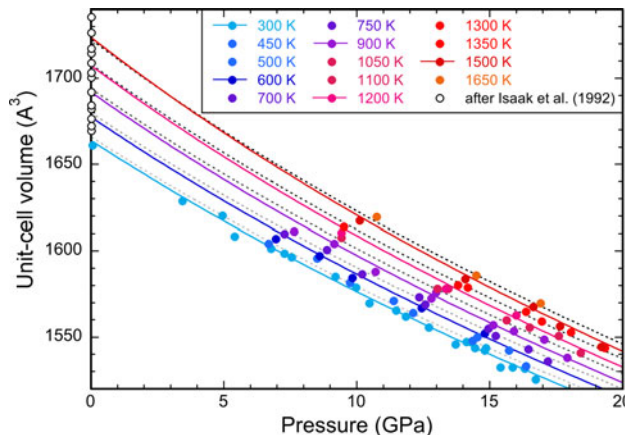


**Fig. 6** Unit-cell volume of  $\text{Ca}_3\text{Al}_2\text{Si}_3\text{O}_{12}$  grossular garnet as a function of pressure and temperature. The errors in the calculation of the pressure are estimated to be  $\pm 0.1$  GPa. However, the error bars have about the same dimension than the symbols and then cannot be seen. The solid lines represent the fit by the high-temperature Birch–Murnaghan equation of state at 300, 600, 900, 1,200 and 1,500 K (all isotherms are not plotted for clarity), with the following parameters:  $K_{0,300} = 166$  GPa,  $K'_{0,300} = 4.03 \pm 0.13$ ,  $V_{0,300} = 1,664 \text{ \AA}^3$  (fixed),  $\alpha_{0,300} = 2.62 \pm 0.23 \times 10^{-5} \text{ K}^{-1}$  and  $(\partial K_{0,T}/\partial T)_P = -0.019 \pm 0.001 \text{ GPa K}^{-1}$  ( $\chi^2 = 1.60$ ). Zero-pressure volume data at high temperature (open circles) are calculated after Isaak et al. (1992). For comparison, dashed line isotherms are plotted after Pavese et al. (2001) at 300, 600, 900, 1,200 and 1,500 K

The thermal pressure is a function of the Grüneisen parameter  $\gamma$  and the thermal energy  $E_{\text{th}}(V, T)$ , which can be estimated using a Debye model (Eq. 7) as shown below:

$$E_{\text{th}}(V, T) = 9nN_A k_B T \left(\frac{\theta}{T}\right)^{-3} \int_0^{\theta/T} \frac{\xi^3}{e^\xi - 1} d\xi \quad (7)$$

where  $\theta$  is the Debye temperature, and the constants  $n$ ,  $N_A$ ,  $k_B$  are the number of atoms in the formula unit ( $n = 20$ ), Avogadro's number ( $6.022 \times 10^{23} \text{ mol}^{-1}$ ) and Boltzmann's constant ( $1.381 \times 10^{-23} \text{ J K}^{-1}$ ), respectively.

The Grüneisen parameter and Debye temperature are usually described as a function of  $\gamma_0$  and  $\theta_0$ , and empirical parameters. Several formulations have been proposed to express  $\gamma$  and  $\theta$ ; here we adopted a unified formulation suggested by Stixrude and Lithgow-Bertelloni (2005). They proposed a thermodynamically consistent formulation for pressure,  $K_T$ ,  $G$  and  $\gamma$ , which are formulated by the derivative of finite strain. The frequencies relative to  $\gamma$ , are assumed to follow a Taylor series expansion in the Eulerian finite strain. The empirical parameter  $q_0$  is introduced in their expression of the volume dependence of the Grüneisen parameter  $\gamma$ . For more details and description of representative equations of  $\gamma$  and  $\theta$ , refer to Stixrude and Lithgow-Bertelloni (2005) and references therein. The Debye temperature at room temperature  $\theta_0 = 823$  (2) K was taken from Anderson and Isaak (1995)'s sound velocity measurements at ambient conditions, and then fixed during refinement of our data. In addition, the bulk modulus  $K_{T0}$  was constrained by the results of the adiabatic bulk modulus measured by acoustic velocity as reported by Bass (1989), using the following relation:

$$K_{T0} = K_{S0} + \gamma_0^2 \rho_0 C_{V0} \times 300 \quad (8)$$

where  $K_{S0}$  is the adiabatic bulk modulus,  $\gamma_0$  is the Grüneisen parameter and  $\rho_0$  the density of grossular at room pressure. The isochoric specific heat at room pressure  $C_{V0}$  was estimated using a Debye function.

Indeed the current data cover the entire high- $P$ ,  $T$  stability field of the grossular garnet, it appears to be not sufficient to constrain  $q_0$  values during fitting. Therefore, here we fixed  $q_0$  and present the results of the fitting for several significant  $q_0$  values as shown in Table 5. As we can see in Table 5, the volume and the bulk modulus at room  $P$  and  $T$  are relatively unaffected by changes in the  $q_0$  value, and then they remain in good agreement with references (Stixrude and Lithgow-Bertelloni 2005). On the other hand, we observe some variation of the pressure derivative of the bulk modulus  $K'_{0,300}$  and the Grüneisen parameter  $\gamma_0$ : if we assume  $q_0 = 0.4$ , our data yield  $\gamma_0 = 1.17$  and  $K'_{0,300} = 4.22$ , which contrast with the values of previous works (Stixrude and Lithgow-Bertelloni 2005). For  $q_0 = 1.0$  (empirical value) and  $q_0 = 1.4$  (as reported for other garnet end-members), our data suggest that  $K'_{0,300}$  is only slightly deviated from 4.0 (as example:  $K'_{0,300} = 4.35$  and  $\gamma_0 = 1.23$  when  $q_0 = 1.4$ ,  $\chi^2 = 1.84$ , Table 5).

## Conclusion

The study of silicate garnet end members at high-pressure and high-temperature is of importance to constrain the

**Table 5** Elastic properties of grossular garnet, compared to previous works as quoted by Stixrude and Lithgow-Bertelloni (2005)

Garnet species	$q_0$	$V_{0,300}$ ( $\text{\AA}^3$ )	$K_{0,300}$ (GPa)	$K'_{0,300}$	$\gamma_0$	$\theta_0^{**}$	$\chi^2$
This study	0	1,662.84	167.3	4.17	1.15	823	1.45
	0.4*	1,662.74	167.2	4.22	1.17	823	1.50
	1.0*	1,662.59	167.2	4.30	1.21	823	1.64
	1.4*	1,662.49	167.1	4.35	1.23	823	1.84
Grossular***							
$\text{Ca}_3\text{Al}_2\text{Si}_3\text{O}_{12}$	0.4 (4)	1,663.59	167 (1)	5.5 (4)	1.08 (6)	823 (2)	–
Pyrope***							
$\text{Mg}_3\text{Al}_2\text{Si}_3\text{O}_{12}$	1.4 (5)	1,503.51	170 (2)	4.1 (3)	1.01 (6)	823 (4)	–
Almandine***							
$\text{Fe}_3\text{Al}_2\text{Si}_3\text{O}_{12}$	1.4 (10)	1,528.62	177 (3)	4.1 (3)	1.10 (6)	742 (5)	–
Mg-majorite***							
$\text{Mg}_3\text{MgSiSi}_3\text{O}_{12}$	1.4 (5)	1,519.99	165 (3)	4.2 (3)	1.01 (30)	788 (100)	–

\* Value is fixed during fitting of the data

\*\*  $\theta_0$  is fixed after Anderson and Isaak (1995)

\*\*\* See Stixrude and Lithgow-Bertelloni (2005) and references therein

compositional dependence of thermoelastic properties in those materials. Such results are particularly valuable for the understanding of natural garnets' behavior at high- $P$ ,  $T$  since they usually display relatively complex composition.

On the basis of the  $P$ - $V$ - $T$  data collected on the beamline BL04B1 at SPring-8 (Hyogo Prefecture, Japan), we calculated the thermal equations of state of synthetic grossular garnet up to 20 GPa and 1,650 K. The high-temperature third order Birch–Murnaghan equation of state gave the following bulk thermoelastic parameters:  $K_{0,300} = 165.4 \pm 0.8$  GPa,  $K'_{0,300} = 4.03 \pm 0.13$ ,  $(\partial K_{0,T}/\partial T)_P = -0.019 \pm 0.001$  GPa  $\text{K}^{-1}$  and  $\alpha_{0,300} = 2.62 \pm 0.23 \times 10^{-5} \text{ K}^{-1}$  ( $\chi^2 = 1.60$ ), with  $V_{0,300}$  fixed to  $1,664 \text{ \AA}^3$ . Fitting of  $P$ - $V$ - $T$  data by the thermal pressure approach using the Mie–Grüneisen–Debye equation of state gave  $K_{0,300} = 167.2$  GPa,  $K'_{0,300} = 4.30$ ,  $V_{0,300} = 1,662.59 \text{ \AA}^3$  and  $\gamma_0 = 1.21$  ( $\chi^2 = 1.64$ ) when  $q_0$  and  $\theta_0$  are fixed to 1.0 and 823 (Isaak et al. 1992), respectively (RMS misfit on pressure of  $\sim 0.3$  GPa).  $\gamma_0$  obtained here for any  $q_0$  value is slightly higher than the value of  $\gamma_0 = 1.08$  quoted by Stixrude and Lithgow-Bertelloni (2005). We note from their compilation that grossular garnet is reported by previous study with high  $K'_{0,300}$  ( $\sim 5.5$ ) and low  $q_0$  ( $\sim 0.4$ ) compared to other garnet end-members ( $K'_{0,300} \approx 4.0$  and  $q_0 \approx 1.4$ ).

The present study constrains  $K'_{0,300}$  of grossular garnet to values in the range of  $K'_{0,300} = 4.03$ – $4.35$ , which well-satisfies thermal expansion data at room pressure (Isaak et al. 1992). Indeed those values differ from other studies for garnets with grossular-like composition (Conrad et al. 1999; Pavese et al. 2001; Zhang et al. 1999), our  $K_{0,300}$  and  $K'_{0,300}$  values also well-reproduce previous and current pressure–volume data for the whole high- $P$ ,  $T$  stability field of grossular

garnet. Thus, the present work supports that  $K'_{0,300}$  of grossular garnet is close to 4.0, which is in contrast to previous works that reported  $K'_{0,300} > 5.0$  (Conrad et al. 1999; Zhang et al. 1999) or  $K'_{0,300}$  close to 3.0 (Pavese et al. 2001). Pavese et al. (2001) fitted  $K'_{0,300}$  close to 3.0 but with large uncertainties that could also satisfy a  $K'_{0,300}$  of 4.0 (Fig. 3). In addition, pressure–volume data of Zhang et al. (1999) and Conrad et al. (1999) can be reproduced by our  $K_{0,300}$  and  $K'_{0,300}$ . Finally, one can note that  $K_{0,300}$  and  $K'_{0,300}$  values reported by computational work for a model of  $\text{Ca}_3\text{Al}_2\text{Si}_3\text{O}_{12}$  garnet show excellent agreement with our results (Nobes et al. 2000). Those results reconcile the thermoelastic parameters of grossular garnet with previous determinations on other silicate garnet species (see Tables 4, 5) as summarized by Stixrude and Lithgow-Bertelloni (2005).

**Acknowledgments** The authors thank T. Inoue, K. Funakoshi, Y. Nishiura, T. Shinmei, Y. Tange and Y. Higo for their helpful assistance in the experiments on BL04B1, at the synchrotron radiation facility, SPring-8 (Project 2009A1300). We are grateful for assistance of H. Ohfuri and A. Yamada in the preparation, observations and analyses of starting materials. We acknowledge A. Pavese and D. Jenkins for their valuable suggestions, which improved the manuscript and C. McCammon for its editorial handling. We thank S. Whitaker for helpful English suggestions. This work was supported by the Global-COE program “Deep Earth Mineralogy”.

## References

- Anderson OL, Isaak DG (1995) Elastic constants of mantle minerals at high temperatures. In: Mineral physics and crystallography: a handbook of physical constants. AGU Reference Shelf 2, Washington, DC, pp 64–97
- Bass JD (1989) Elasticity of grossular and spessartite garnets by Brillouin spectroscopy. J Geophys Res 94:7621–7628

- Bass JD, Anderson DL (1984) Composition of the upper mantle: geophysical tests of two petrological models. *Geophys Res Lett* 11:229–232
- Conrad PG, Zha CS, Mao HK, Hemley RJ (1999) The high-pressure, single-crystal elasticity of pyrope, grossular, and andradite. *Am Mineral* 84:374–383
- Deuss A, Redfern SAT, Chambers K, Woodhouse JH (2006) The nature of the 660-kilometer discontinuity in Earth's mantle from global seismic observations of PP precursors. *Science* 311:198–201
- Fan DW, Zhou WG, Liu CQ, Liu YG, Wan F, Xing YS, Liu J, Bai LG, Xie HS (2009) The thermal equation of state of  $(\text{Fe}_{0.86}\text{Mg}_{0.07}\text{Mn}_{0.07})_3\text{Al}_2\text{Si}_3\text{O}_{12}$  almandine. *Mineral Mag* 73(1):95–102
- Hazen RM, Finger LW (1978) Crystal structures and compressibilities of pyrope and grossular to 60 kbar. *Am Mineral* 63:297–303
- Higo Y, Kono Y, Inoue T, Irfune T, Funakoshi KI (2009) A system for measuring elastic wave velocity under high pressure and high temperature using a combination of ultrasonic measurement and the multi-anvil apparatus at SPring-8. *J Synchrot Radiat* 16:762–768
- Irfune T, Ringwood AE (1987) Phase transformation in a harzburgite composition to 26 GPa: Implication for dynamical behavior of the subducting slab. *Earth Planet Sci Lett* 86:365–376
- Irfune T, Ringwood AE (1993) Phase transformation in subducted oceanic crust and buoyancy relationships at depths of 600–800 km in the mantle. *Earth Planet Sci Lett* 117:101–110
- Isaak DG, Anderson OL, Oda H (1992) High-temperature thermal expansion and elasticity of calcium-rich garnets. *Phys Chem Min* 19:106–120
- Jackson I, Rigden SM (1996) Analysis of  $P$ – $V$ – $T$  data: Constraints on the thermoelastic properties of high-pressure minerals. *Phys Earth Planet Int* 96:85–112
- Larson AC, Von Dreele RB (2000) GSAS general structure analysis system operation manual. Los Alamos National Laboratory LAUR 86–748:1–179
- Le Bail A, Duroy H, Fourquet JL (1988) Ab initio structure determination of  $\text{LiSbWO}_6$  by X-ray powder diffraction. *Mater Res Bull* 23:447–452
- Meagher EP (1975) The crystal structures of pyrope and grossularite at elevated temperatures. *Am Mineral* 60:218–228
- Nobes RH, Akhmatkaya EV, Milman V, Winkler B, Pickard CJ (2000) Structure and properties of aluminosilicate garnets and katoite: an ab initio study. *Comput Mater Sci* 17:141–145
- Novak GA, Gibbs GV (1971) The crystal chemistry of the silicate garnets. *Am Mineral* 56:791–825
- Olijnyk H, Paris E, Geiger CA, Lager GA (1991) Compressional study of katoite  $[\text{Ca}_3\text{Al}_2(\text{O}_4\text{H}_4)_3]$  and grossular garnet. *J Geophys Res* 96
- Osborn EF, Muan A (1960) The system  $\text{CaO}-\text{Al}_2\text{O}_3-\text{SiO}_2$ . Plate No. 1 in phase equilibrium diagrams of oxide systems 219
- Pavese A, Diella V, Pischedda V, Merli M, Bocchio R, Mezouar M (2001) Pressure-volume-temperature equation of state of andradite and grossular, by high-pressure and -temperature powder diffraction. *Phys Chem Min* 28:242–248
- Rodehorst U, Geiger CA, Armbruster T (2002) The crystal structures of grossular and spessartine between 100 and 600 K and the crystal chemistry of grossular-spessartine solid solutions. *Am Mineral* 87:542–549
- Rubie DC (1998) Characterising the sample environment in multianvil high-pressure experiments. *Phase Transit* 68:431–451
- Saikia A, Frost DJ, Rubie DC (2008) Splitting of the 520-kilometer seismic discontinuity and chemical heterogeneity in the mantle. *Science* 319:1515–1518
- Sawada H (1999) Electron Density Study of Garnets:  $Z_3\text{Al}_2\text{Si}_3\text{O}_{12}$  ( $Z = \text{Mg}, \text{Fe}, \text{Mn}, \text{Ca}$ ) and  $\text{Ca}_3\text{Fe}_2\text{Si}_3\text{O}_{12}$ . *J Solid State Chem* 142:273–278
- Karato S, Wang Z, Liu B, Fujino K (1995) Plastic deformation of garnets: systematics and implications for the rheology of the mantle transition zone. *Earth Planet Sci Lett* 130:13–30
- Skinner BJ (1956) Physical properties of end-members of the garnet group. *Am Mineral* 41:428–436
- Stixrude L, Lithgow-Bertelloni C (2005) Thermodynamics of mantle minerals—I. Physical properties. *Geophys J Int* 162:610–632
- Thiéblot L, Roux J, Richet P (1998) High-temperature thermal expansion and decomposition of garnets. *Eur J Mineral* 10:7–15
- Thiéblot L, Téqui C, Richet P (1999) High-temperature heat capacity of grossular ( $\text{Ca}_3\text{Al}_2\text{Si}_3\text{O}_{12}$ ), enstatite ( $\text{MgSiO}_3$ ), and titanite ( $\text{CaTiSiO}_5$ ). *Am Mineral* 84:848–855
- Toby BH (2001) EXPGUI, a graphical user interface for GSAS. *J Appl Crystallogr* 34:210–213
- Tsuchiya T (2003) First-principles prediction of the  $P$ – $V$ – $T$  equation of state of gold and the 660-km discontinuity in Earth's mantle. *J Geophys Res B Solid Earth* 108
- Wang Y, Weidner DJ, Zhang J, Gwanmesia GD, Liebermann RC (1998) Thermal equation of state of garnets along the pyrope-majorite join. *Phys Earth Planet Int* 105(1–2):59–71
- Zhang L, Ahsbahs H, Kutoglu A, Geiger CA (1999) Single-crystal hydrostatic compression of synthetic pyrope, almandine, spessartine, grossular and andradite garnets at high pressures. *Phys Chem Min* 27:52–58